IEEE Access
Multidisciplinary | Rapid Review | Open Access Journal

Received April 21, 2020, accepted May 12, 2020, date of publication May 27, 2020, date of current version June 9, 2020.

Digital Object Identifier 10.1109/ACCESS.2020.2997933

Active Reconfigurable Ultra-Wideband Antenna With Complementary Frequency Notched and Narrowband Response

CHINMOY SAHA[1], (Senior Member, IEEE), JAWAD Y. SIDDIQUI[2,4], (Senior Member, IEEE), A. P. FREUNDORFER[3], (Senior Member, IEEE), LATHEEF A SHAIK[1], (Member, IEEE), AND Y. M. M. ANTAR[4], (Life Fellow, IEEE)

[1]Indian Institute of Space Science and Technology, Thiruvananthapuram 695547, India
[2]Institute of Radio Physics and Electronics, University of Calcutta, Kolkata 80523, India
[3]Department of ECE, Queen's University, Kingston, ON K7L3N6, Canada
[4]Department of ECE, Royal Military College of Canada, Kingston, ON K7K7B4, Canada

Corresponding author: Chinmoy Saha (csaha@ieee.org)

The work of Chinmoy Saha was supported by the Science and Engineering Research Board (SERB), Department of Science and Technology, Government of India, under the DST Core Grant Scheme under Grant CRG/2019/004570).

ABSTRACT An active reconfigurable ultra-wideband antenna exhibiting complementary frequency notched and narrowband responses is proposed in this paper. The frequency responses are achieved on a CPW fed single element printed monopole antenna loaded with a pair of split ring resonators (SRR) and PIN Diodes. The SRRs and PIN Diodes embedded on the Coplanar Waveguide (CPW) feed works as an inline filter, when activated, exhibits frequency reconfigurability by transforming a frequency notched wideband antenna into a narrowband antenna. Different biasing conditions (reverse and forward) on the loaded PIN diodes toggle between frequency-notched and narrow band response of the antenna. Prototypes are fabricated and the measured impedance and radiation characteristics are presented. This concept offers multi-antenna functionality using a single radiator without any modification or addition to the radiator geometry.

INDEX TERMS Active antenna, frequency notch antenna, PIN diodes, UWB antenna, cognitive radio.

I. INTRODUCTION

Modern RF systems employ transceivers which comprise multiple antennas for different functions and applications. Reconfigurable printed antennas are desirable in such wireless systems which can alleviate the undesired co-housing of multiple antennas [1]. Reconfigurable antennas have been studied by numerous research groups over last few decades and a good account of the works are compiled in [2]. Reconfiguration techniques in a reconfigurable antenna, as indicated in Figure 1, can be broadly classified into four categories: i) electrical reconfiguration, ii) optical reconfiguration, iii) physical reconfiguration, iv) material based reconfiguration [2], [3]. One of the recent techniques of achieving antenna reconfigurability is cascading a reconfigurable filter section in the feed line of the printed antennas. By this technique, a single antenna can be operated to work in different bands or different operating frequencies [4]–[7]. Figure 2 shows a basic block diagram of such reconfigurable filtered based antenna. One such integrated antenna-filter combination, where a reconfigurable bandpass

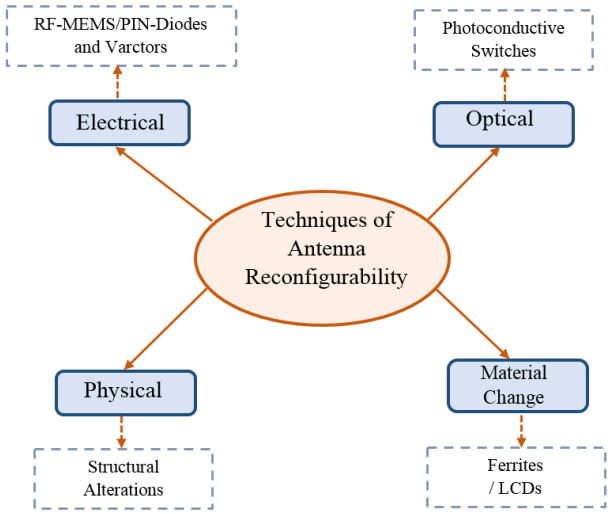

FIGURE 1. Various techniques of achieving antenna reconfigurability.

The associate editor coordinating the review of this manuscript and approving it for publication was Santi C. Pavone.

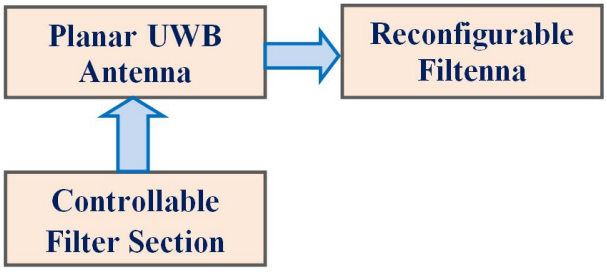

FIGURE 2. Block Diagram of the proposed planar antenna based reconfigurable filtenna.

filter is incorporated within the feeding line of a printed antenna, is referred to as a filtenna in [8]. A recent paper showing a compact broadband reconfigurable frequency tunable structure using single ring rectangular shaped SRRs coupled to a CPW line provides a stop-band in the transmission characteristic of the line [9]. The structure can also be reconfigured from band-stop to band-pass configuration by switching the loaded pair of p-i-n diodes across slots of the host CPW [9]. When an additional PIN diode is connected between the two rectangular rings placed beneath the respective slots of the CPW in a diagonal fashion, it effectively acts like a new S-shaped SRR with enhanced length and thereby provides a new resonance frequency as also shown in the paper [9]. Table-1 presents a comprehensive summary of various reconfigurable UWB antennas [8], [10]–[23] reported over last few years.

In this paper, a multi-functional and reconfigurable antenna is realized using the design concept presented in [9] and [24]. A pair of SRRs and PIN diode loaded in the CPW feed line constitute a dual state filter section, exhibiting frequency-notched/narrow band-pass response depending on the status (ON/OFF) of the PIN diode. This filter section can be integrated in the feed-section of any CPW fed antenna. The present antenna, due to this integrated dual state filter section, exhibits a unique frequency reconfiguration capability that transforms a frequency notched wideband antenna into a narrowband antenna where the narrowband frequency complements the notch frequency. A single printed monopole antenna loaded with SRRs and PIN diodes on the feed section provides the dual functionality. Here, unlike in [9], the SRRs used are square shaped and no additional PIN/varactors diodes are connected between them. The frequency notch in the wideband printed monopole antenna is caused by the SRRs which are magnetically coupled with feeding CPW line and inhibit signal propagation around the SRRs' resonance frequency [24]–[26]. With the loading of PIN diodes on CPW and appropriate biasing, the frequency notched wideband antenna can be reconfigured into a narrowband antenna operating at the SRR's resonance. The design is realized using a printed circular monopole antenna having a wide bandwidth. The printed monopole is fed by a CPW transmission line loaded with a pair of SRRs and PIN diodes.

It is further demonstrated that the notch frequency and the narrowband frequency can be tuned by changing the physical dimension of the SRR geometry as well as shape of the SRRs without perturbing the radiator dimension. The various shapes of SRRs that can be utilized are circular, square, hexagonal and triangular. Moreover, the inclusion of the SRRs and the PIN diodes on the feed section of the antenna do not have any adverse impact on the radiation performance of the antenna. Physical insight of the dual functionality is explained using the simulated contour Poynting vector plots. Potent application of such reconfigurable antennas are, i) MIMO systems used for high-data rate applications, ii) cognitive radio (CR) systems of Software Defined Radio (SDR) which demand wideband and narrowband antennas [27], iii) multiservice/multiband/multi-standard radio (MSR).

The paper is organized as follows: Sec. II describes the realization of the dual state filter. Section III deals with the design and development of the proposed dual complimentary response based CPW fed monopole antenna. Antenna configurations and corresponding simulated and measured results are reported in section IV. This section also presents some physically insightful plots obtained from [28] which sheds more light on the principle of operation of the proposed antenna and are in confirmation with the measured results. The paper is concluded in Sec. V.

II. REALIZATION OF DUAL STATE FILTER SECTION

Proposed active reconfigurable antenna design achieves reconfiguration features due to the reconfigurable filter section integrated in the feed-line of the antenna. This makes the design of the filter-section and the radiator mutually independent which allows the proposed concept to be easily extended to any other printed antenna. In this section, a very brief description on the realization of the dual-state filter section is discussed. Section–III employs this filter section in a printed monopole antenna which effectively converts the antenna into a reconfigurable filtenna. The dual state filter section is realized by loading a pair of square-shaped SRRs beneath the slot lines of a 50 Ω CPW line and a pair of PIN diodes connected between the signal lines and ground lines of the CPW. To ensure best possible excitation of the SRRs by the propagating magnetic field of the CPW line, SRRs are precisely located so that centre of the SRRs falls on the centre of the slots of the CPW. Figure 3 shows the fabricated prototypes of such a dual state filter. The SRRs having dimension of $a_{\text{ext}} = 2.5$ mm, $c = 0.35$ mm, $d = 0.7$ mm and $g_1 = g_2 = 0.4$ mm (see fig. 6(c) for notations)are printed on RT-Duriod 5870 laminate with $\varepsilon_r = 2.33$ and $tan\delta = 0.0009$ with precise location. A pair of silicon PIN diodes with model no. SMP 1145 are placed on the opposite side of substrate. When the diodes are not biased, due to the resonance of the SRR, the SRR loaded CPW yield band-notched function. On the other hand, with suitable forward bias voltage, the combination of SRRs and PIN-diodes acting as 'ON' switch constitute a narrow BPF. Figure 4 shows the experimental set up for characterizing the S-parameters of the SRRs and PIN diode loaded filter section.As indicated in Fig. 4, PIN diodes are biased ON/OFF

TABLE 1. Comprehensive survey of the existing reconfigurable antennas.

Ref.	Antenna Functionality	Means of Reconfiguration	No of switching/tuning elements used	Antenna Type	Antenna Size (mm×mm)	Frequency Range GHz
[8]	Tuning the operating frequency	Varactor	One varactor	Dual sided vivaldi	59.8 × 30	6.1-6.5
[10]	Dual band selected through PIN diode and tuned with varactor	Varactor and PIN diode	1 varactor and 1 PIN	Meandered and U-shaped monopole	11.5 × 8.4	2.39-3.0
[11]	UWB for sensing and narrow band for communicating	Photoconductive silicon switches	4 Switches	U-shaped monopole and open annulus	40 × 38.5	3.1-10.6 and 5.8-6.8, 6.7-7.3, 7.0-8.4, 7.9-9.2
[12]	Wideband or four different narrowband operations	PIN diode	2 PIN diode	CPW fed monopole	80 × 60	1.3-6, 2.55, 2.6, 2.8, 3.2GHz
[13]	Wideband and narrowband	Reconfigurable Filter section in the feed-line	1 PIN and 2 varactor	Circular disc monopole	60×30	3.8-6, 3.9-4.82
[14]	Wideband and tunable narrowband	Varactor and PIN diode	2 varactor and 1 PIN	Funnel shaped monopole	50 × 30	2.4-5, NB tuned between 3.0-4.4GHz
[15]	Wideband and two narrow bands	PIN diode	5 PIN diodes	Elliptical shaped monopole	45 × 40	2.2-11, 2.4-2.6, 5-6.2GHz
[16]	One wideband and four narrow-bands	PIN diode	4 PIN diodes	Folded bow-tie dipole, thin dipole and loop	3D antenna	0.83-2.16 and 0.9, 1.15, 1.5 and 1.85
[17]	Two wide-bands (extending the BW of 1st band)	PIN diode	2 PIN diodes	Slot antenna	24.6 × 8.6	5.2, 5.5
[18]	Two different antenna (one employs varactor and other PIN diode)	Varactor and PIN diode	2 varactor and 6 PIN diodes	Printed folded dipoles	NA	Ant1: 6-6.6 Ant 2:5.3-6.6 and 6.4-8
[19]	Five narrow-bands	Motorized rotation of substrate	Motor	Printed monopole and multiple patches	70 × 50	3.4-5.56, 6.3-10, 2.1-3, 5.4-6.2, 3-3.4
[20]	Converting wideband antenna to 4 different narrowband antennas	GaAs FET switch	Two SPDT switched	Circular monopole	50 × 50	2-11, 2.1-2.6, 3.6-4.6, 2.8-3.4 and 4.9-5.8
[21]	Tuning the operating frequency	Varactor and motion actuation	One varactor	Dual sided vivaldi	59.8 × 30	6.6-7.2
[22]	Converting wideband antenna to four different narrowband antennas	PIN diodes	12 PIN diodes	Inverted U-shaped patch	68×51	2.5-3.75
[23]	Reconfigurable MIMO	Varactors and PIN diodes	4 PIN and 2 Varactor	UWB monopole and meandered line monopole	65 × 120	0.72-3.44

using a DC bias source applied through the in-built bias Tee of the VNA which also ensures isolation of DC and RF. Figure 5(a) and (b) shows the measured S-parameters of the realized CPW based reconfigurable filter for the PIN diode in OFF and ON state respectively. As indicated in Fig 5(a), with diodes in OFF state the prototype yields band-notched response. The same prototype, with the PIN diode in ON state exhibits a narrow pass-band response. Thus, the SRR and PIN diode loaded CPW can act as a dual state reconfigurable filter.

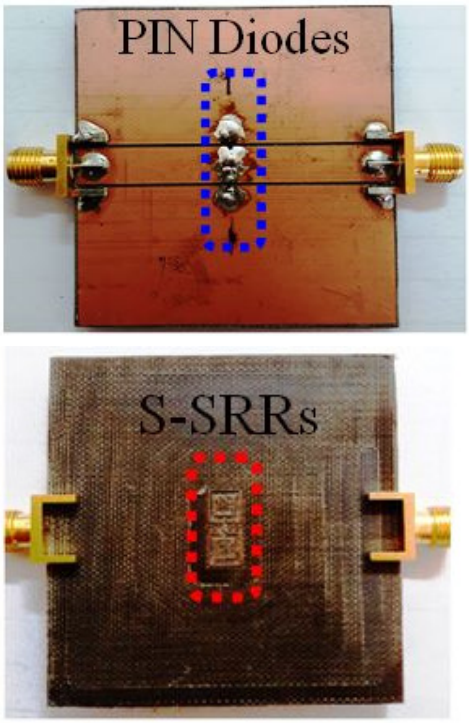

FIGURE 3. Fabricated prototype of the PIN-diode actuated S-SRR loaded CPW based dual state reconfigurable filter.

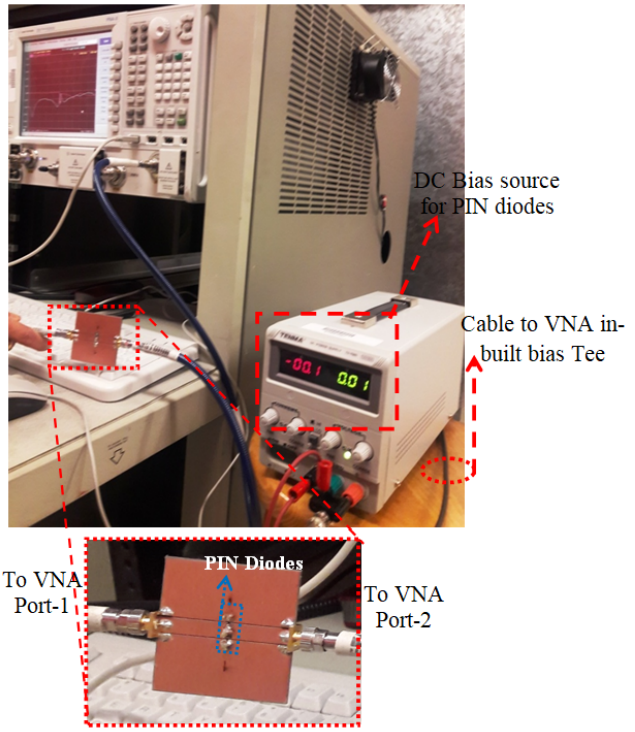

FIGURE 4. Experimental setup for characterizing the dual state filter with bias source and in-built bias Tee.

III. ANTENNA CONFIGURATION

Figure 6 shows the schematic of the proposed active antenna loaded with SRRs and PIN diodes on the CPW feed section. A circular monopole having radius R is fed by a CPW line consisting of ground planes having width W_1 and W_2, length Ls and a signal line of width S and length $Ls + t$.

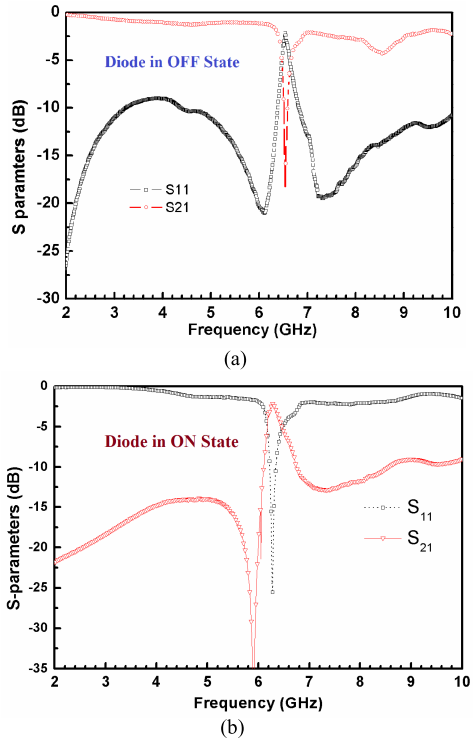

FIGURE 5. Measured S-parameters of the realized dual-state filter section.

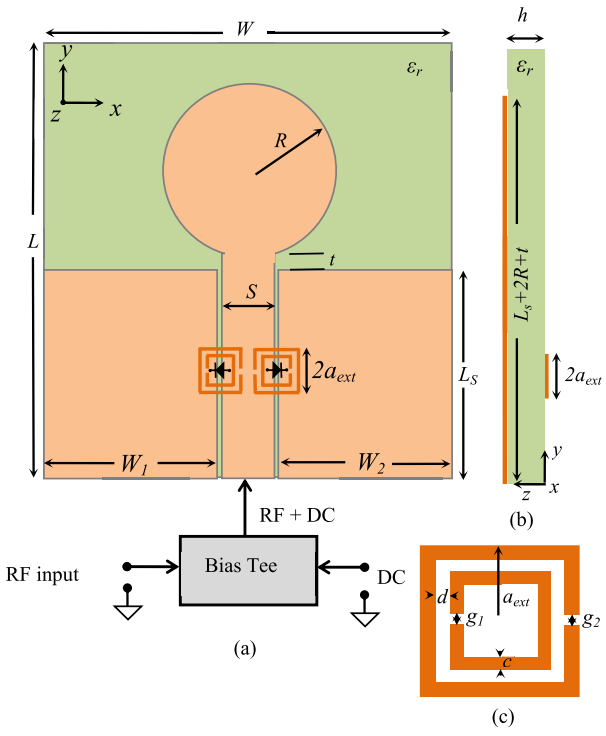

FIGURE 6. Schematic of SRR coupled PIN diode loaded active antenna (a) Top view of CPW fed printed circular monopole connected to external bias tee with a pair of SRRs printed on the back side and a pair of PIN diodes on the CPW slots. (b) Side View showing the printed SRRs separated by *h* from the PIN diode loaded CPW feed line. (c) Schematic of a unit cell of square SRR, a pair of which is printed on the back side of the CPW feed line and aligned with the PIN diodes.

The signal line and the ground planes are separated by a symmetric pair of slot gaps, s_g. The antenna is printed on a substrate having thickness h and dielectric constant ε_r. Two square shaped split ring resonators having dimension, a_{ext}, which is half the dimension of the side-length of the SRR, conductor thickness c, separation between rings d and split gaps g_1 and g_2 as shown in Fig. 6(c), are printed on the other side of the substrate with their centers coinciding with the slot lines of the CPW feed. A pair of PIN diodes are placed on the slots of the CPW with their positions coinciding with the axes passing through the center of the SRRs.

In the proposed configuration, the CPW is inductively coupled to a pair of SRRs, having narrow split gaps g_1 and g_2, which are symmetrically placed on the backside of the substrate. The propagating electric field vector is polarized along the plane of the SRRs and the magnetic field vector is polarized along the SRRs' axes. The propagating signal excites the SRR, which prohibits transmission around its resonance frequency determined by the SRRs' dimensions and the constitutive parameters of the host substrate yielding in frequency notch [26]. The symmetric position of the SRRs to optimize efficient magnetic coupling has been shown to yield notch in the antenna impedance and radiation characteristic [26], [29], [30].The CPW transmission line also being loaded with PIN diodes which on different biasing conditions (reverse and forward) would effectively open and short the signal line with the ground planes. This, in turn provides frequency notched response and its complementary narrow band response.

The prototype was fabricated on Taconic substrate having $\varepsilon_r = 2.33$, $tan\ \delta = 0.0009$ and thickness $h = 1.575$mm. The circular monopole having radius $R = 12.5$mm and fed with a CPW having ground plane length $L_s = 22.5$ mm, width $W = 50$mm, signal line width $S = 6$mm, slot gap $S_g = 0.3$mm and feed gap $t = 0.2$mm was etched on one side of the substrate. The slot gaps and the signal line width were optimized to yield a line impedance close to 50Ω. A pair of SRRs having dimensions $a_{ext} = 2.5$mm, $c = 0.35$ mm, $d = 0.6$ mm and split gaps $g_1 = g_2 = 0.5$ mm, were printed on the other side of the substrate with their axes coinciding with the slot line in the CPW as shown in Fig. 7. A pair of silicon PIN diodes (SMP 1145) were placed on the slots between the ground planes and the signal line and aligned to the position of SRRs axes. As shown in Fig. 7(b), the required DC bias to the diodes are provided using a Mini circuits 15542 bias tee.

IV. MEASUREMENTS AND RESULTS

The proposed SRR and PIN diode loaded active antenna is simulated using a commercial electromagnetic simulator [28]. In this simulation two different configuration of the active antenna for ON and OFF state of the diodes are considered by replacing the diodes with the corresponding equivalent circuits as shown in Fig. 8. The lumped circuit parameters, obtained from the manufacturer's data sheet, in diode ON condition assigned in the simulation were

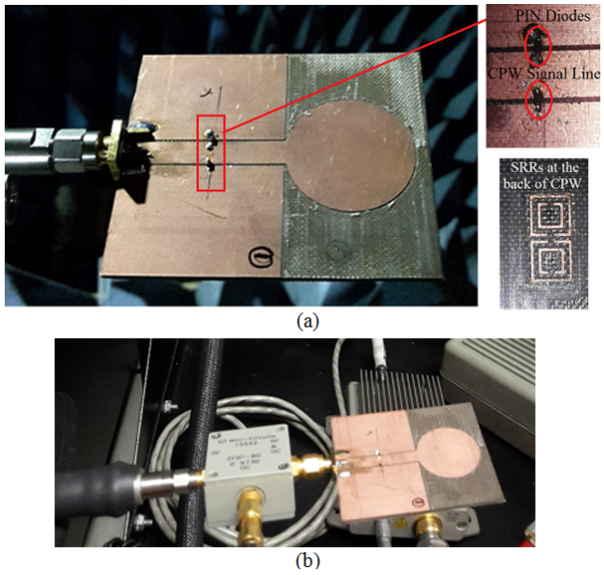

FIGURE 7. (a) Fabricated prototype of the proposed active antenna with a magnified view of the PIN diodes accommodated between the signal line and ground planes of the CPW. SRRs are printed on the opposite side of the CPW (b) Prototype connected to the Mini Circuits bias Tee.

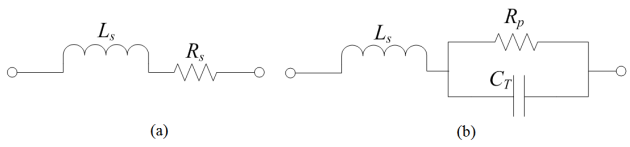

FIGURE 8. Lumped equivalent circuit of the PIN diode (a) ON (b) OFF.

$L_s = 0.45$nH and $R_s = 2\Omega$ and in diode OFF condition were $L_s = 0.45$nH and $R_p = 5$MΩ and $C_T = 0.14$fF. The resultant HFSS model with lumped circuit parameters for both the cases are simulated. Figure 9 shows the simulated and measured S_{11} plots of the proposed active antenna for OFF status of the diode. The plot indicates wideband characteristic from 2.5 GHz to 11 GHz with a sharp notch at 6.1 GHz and 6.01 GHz for simulated and measured data, respectively. This notch corresponds to the resonance frequency of the SRR and can be varied by scaling the physical dimension of the SRRs [26]. The variation between simulation and measurement post-resonance is due to the ohmic loss arising from the finite impedance of the PIN diodes in their OFF state.

Figure 10 shows the simulated and measured S_{11} of the prototype active antenna with the diode in ON condition. As revealed in the plot, with the diode in ON condition, the antenna yields a narrowband response centered at 6.12 GHz and 6.02 GHz for simulated and measured data and effectively complements the impedance behavior of the antenna in diode OFF condition. Figures 9 and 10 reveal the complementary nature of the antenna under diode OFF and ON conditions. The active antenna with diode ON condition provides a narrow band response due to the narrow band pass filter formed with the combination of SRRs and PIN diodes on the slots of the CPW. On the other hand, with diode in OFF condition, the band notch filtering of the SRRs contribute to

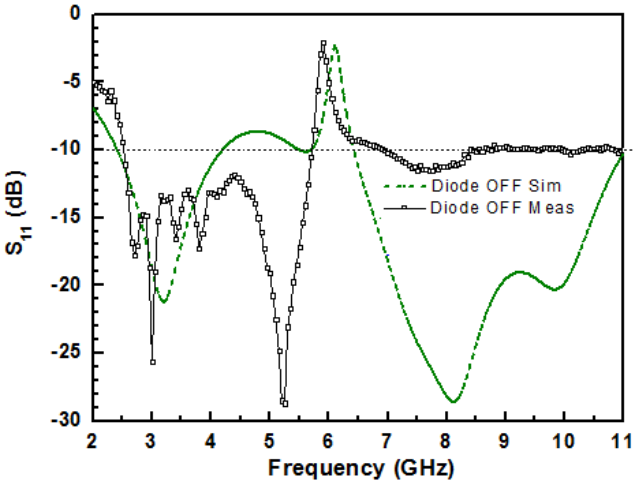

FIGURE 9. Measured and simulated S_{11} response of the SRR coupled PIN diode loaded CPW fed printed circular monopole active antenna with diodes in OFF conditions. $\varepsilon_r = 2.33$, thickness $h = 1.575$mm, $R = 12.5$mm, $L_s = 22.5$ mm, $W = 50$mm, $S = 6$mm, $S_g = 0.3$mm, $t = 0.2$mm; SRR parameters: $a_{ext} = 2.5$ mm, $c = 0.35$ mm, $d = 0.6$ mm and split gaps, $g_1 = g_2 = 0.5$ mm.

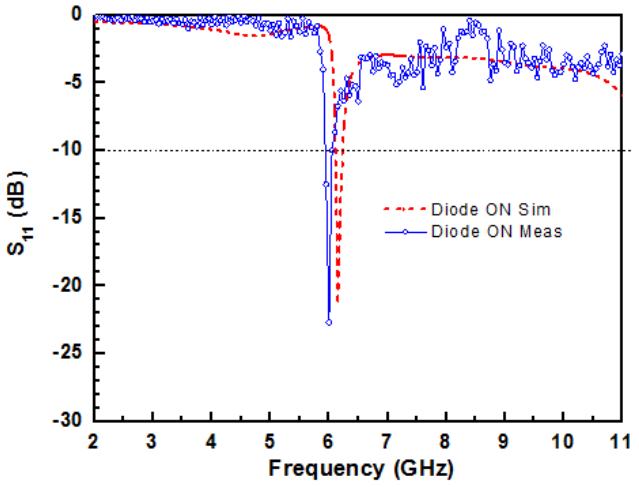

FIGURE 10. Measured and simulated S_{11} response of the SRR coupled PIN diode loaded CPW fed printed circular monopole active antenna with diodes in ON conditions. Parameters as in Fig. 9.

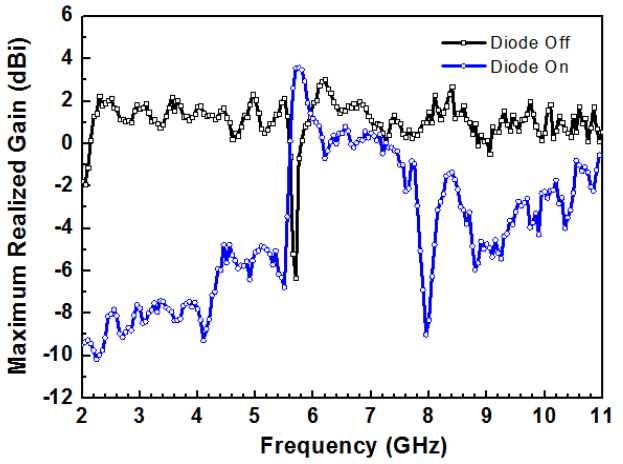

FIGURE 11. Measured realized peak gain of the SRR coupled PIN diode loaded CPW fed printed circular monopole active antenna with diodes OFF and ON conditions. Parameters as in Fig. 9.

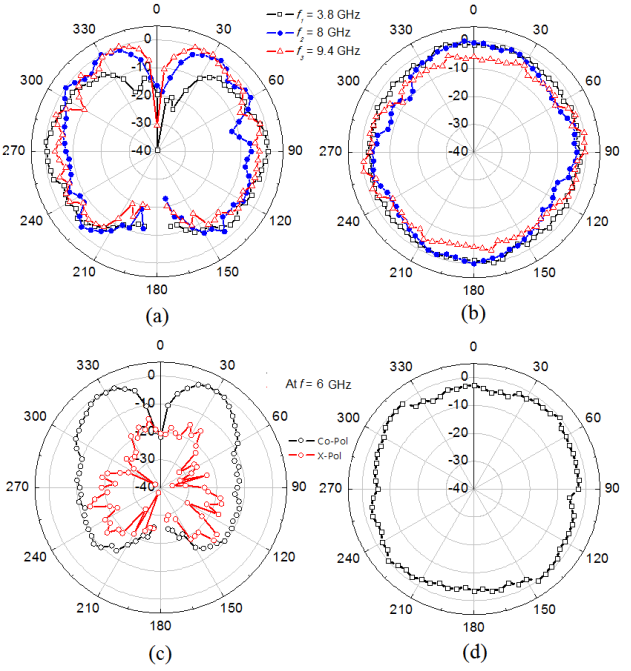

FIGURE 12. Measured normalized E and H-plane radiation patterns of the fabricated active antenna. (a) and (c) x-y plane (E-plane) in diode OFF and ON conditions. (b) and (d) x-z plane (H-plane) in diodes OFF and ON condition.

frequency notched UWB response of the antenna. The biasing of the diodes is conducted through 5V D.C. supply connected to the bias tee. The current flowing through the diodes in forward bias condition provides the DC-short between signal and ground planes of the CPW which in turn reconfigures the notched wideband antenna into a narrowband antenna.

Figure 11 shows the measured maximum realized peak gain plotted against the frequency of the prototype active antenna in diode OFF and ON conditions. In diode OFF condition, the gain drops sharply at the notch frequency of 6.01 GHz prohibiting radiation whereas for the rest of the frequencies the gain remains above 0 dBi. A complementary gain profile is yielded when the diode is switched ON and the gain rises sharply at 6.02 GHz and drops off at either side of the radiating frequency. The measured gain value in diode ON condition at the narrowband frequency 6.02 GHz was obtained as 3.59 dBi.

The measured normalized radiation patterns in two principal planes, the *x*-*y*-plane (E-plane) and *x*-*z*-plane (H-plane), for the prototype in diodes OFF condition are shown in Fig. 12(a) and 12(b), respectively, for 3.8 GHz, 8 GHz and 9.4 GHz. The E-plane and H-plane at 6.02 GHz for diode ON condition are shown in Fig. 12(c) and 12(d). The radiation patterns indicate axial null along *y*-axis ensuring monopole type radiation for the *x*-*y* -plane with high cross polar discrimination. The H-plane radiation yields an omni-directional pattern for the *x*-*z*-plane. The simulated efficiency was obtained

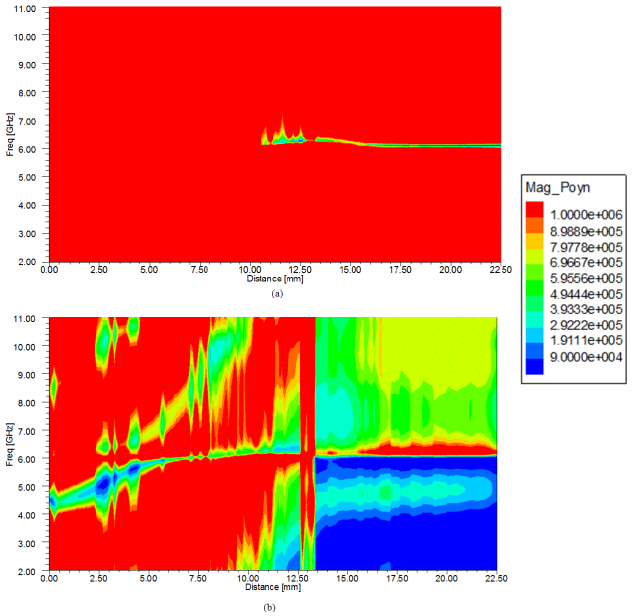

FIGURE 13. Simulated contour plots of the magnitude of the Poynting vectors through one of the CPW slots as a function of frequency. (a) with diodes OFF condition and (b)with diodes ON condition. (Plots are in uniform scale).

at 92% and 76% for diode OFF and diode ON conditions, respectively.

A more physical insight of the complementary nature of the antenna response can be arrived by observing the magnitude of the Poynting vector along the feed-line in diode ON and diode OFF conditions as illustrated in Fig. 13.The figure represents a 3D contour plot with x-axis being the distance from the connector to the radiator and y-axis representing the frequency and color coding represents the pointing vector, plotted using field calculator option of 3D EM solver [28]. As shown in Fig. 13(a), with the diode in OFF condition, the SRR prohibits propagation of electromagnetic energy at its resonance frequency yielding a notched UWB response. Before the SRR location electromagnetic energy of all frequencies propagating, after interaction with SRR one frequency is prohibited from reaching the radiator. With the diode in ON condition, a complementary nature of the propagation is triggered where electromagnetic energy over only a narrow frequency at approximately the SRRs resonance frequency band is propagated. The rest of the energy is reflected back to the input port as depicted in Fig. 13(b).

Figure 14 shows the simulated reflection coefficient of the proposed antenna for different a_{ext} dimensions in diode ON and diode OFF conditions. Three different a_{ext} dimensions of 2.3mm, 2.5mm and 2.7mm yielded notch frequencies in diode OFF condition at 5.45 GHz, 6.1 GHz and 6.65 GHz while with diode in ON condition narrowband response centered at 5.5 GHz, 6.15 GHz and 6.7GHz is obtained. Figure 14 has an inset which shows the zoomed view of the notch and narrowband frequencies from 5GHz to 7GHz to increase the legibility. The wide variation of the notch and narrowband frequency using the proposed concept by

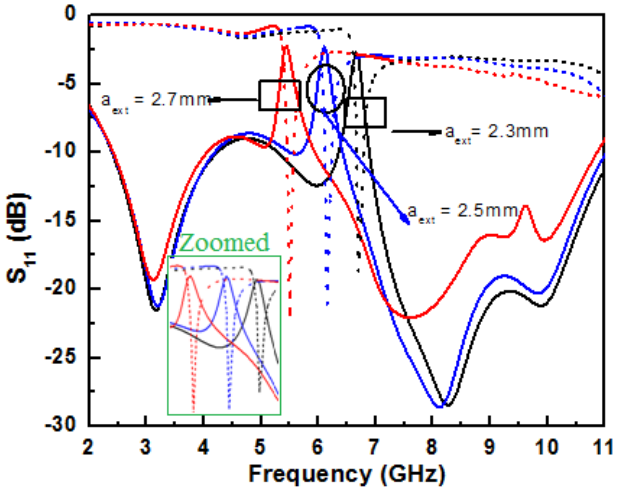

FIGURE 14. Simulated S_{11} of the SRR coupled PIN diode loaded CPW fed printed circular monopole active antenna with diodes OFF and ON conditions for various a_{ext} values. Solid curves are for diode OFF case and dotted curves are for diode ON case.

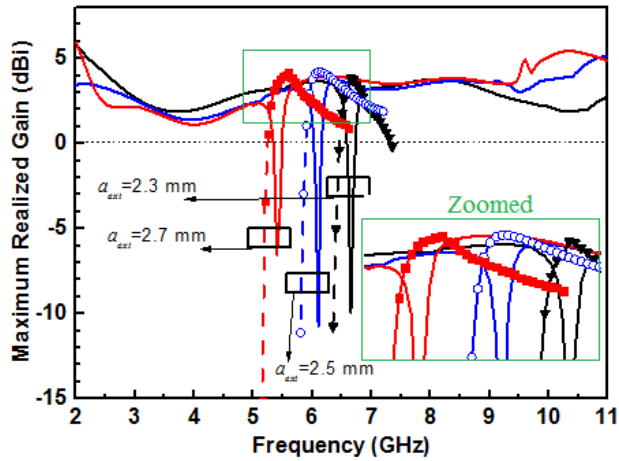

FIGURE 15. Simulated realized peak gain of the SRR coupled PIN diode loaded CPW fed printed circular monopole active antenna with diodes OFF and ON conditions for various a_{ext} values. Solid curves are for diode OFF case and dotted curves are for diode ON case conditions.

changing the SRR parameter and without altering the basic radiator dimension is evident from the figure. Similar variation can also be achieved by changing the other parameters of the SRRs like c, d and g. The corresponding simulated maximum realized gain as a function of frequency of SRRs with varying a_{ext} is shown in Fig. 15. The dip and peak in gain parameters in diode OFF and ON conditions are evident from the plots.

V. CONCLUSION

A novel active reconfigurable UWB antenna with real time switching yielding complementary responses of frequency notched wideband and narrowband is realized and validated in this paper. The multiple frequency reconfigurability is achieved by loading the CPW transmission line with a pair of SRRs and PIN diodes. The combination of the SRRs with different conditions of diode bias yield the two complementary characteristics. Prototype was fabricated to

validate the simulated results with the measured impedance and radiation characteristics. Since the notch and narrow band frequency is determined by the SRRs geometry, several multi-dimensional SRRs can be used for multiple frequency notches. The antenna can be replaced with any other sensor which would yield the desired response using the proposed technique.

REFERENCES

[1] C. A. Balanis, *Modern Antenna Handbook*. Hoboken, NJ, USA: Wiley, 2008.

[2] J. T. Bernhard, "Reconfigurable antennas," in *Synthesis Lectures on Antennas*, C. A Balanis, Ed San Rafael, CA, USA: Morgan & Claypool, 2007, pp. 1–66.

[3] C. G. Christodoulou, Y. Tawk, S. A. Lane, and S. R. Erwin, "Reconfigurable antennas for wireless and space applications," *Proc. IEEE*, vol. 100, no. 7, pp. 2250–2261, Apr. 2012.

[4] D. E. Anagnostou, "Design, fabrication, and measurements of an RF-MEMS-based self-similar reconfigurable antenna," *IEEE Trans. Antennas Propag.*, vol. 54, no. 2, pp. 422–432, Feb. 2006.

[5] D. E. Anagnostou, M. T. Chryssomallis, B. D. Braaten, J. L. Ebel, and N. Sepúlveda, "Reconfigurable UWB antenna with RF-MEMS for on-demand WLAN rejection," *IEEE Trans. Antennas Propag.*, vol. 62, no. 2, pp. 602–608, Feb. 2014.

[6] S. A. Aghdam, "A novel UWB monopole antenna with tunable notched behavior using varactor diode," *IEEE Antennas Wireless Propag. Lett.*, vol. 13, pp. 1243–1246, 2014.

[7] M. S. Khan, A. D. Capobianco, A. Naqvi, M. F. Shafique, B. Ijaz, and B. D. Braaten, "Compact planar UWB MIMO antenna with on-demand WLAN rejection," *Electron Lett.*, vol. 51, no. 13, pp. 963–964, 2015.

[8] Y. Tawk, J. Constantine, and C. G. Christodoulou, "A varactor-based reconfigurable filtenna," *IEEE Antennas Wireless Propag. Lett.*, vol. 11, pp. 716–718, 2012.

[9] A. K. Horestami, Z. Shaterian, J. Naqui, F. Martin, and C. Fumeaux, "Reconfigurable and tunable S-shaped split-ring resonators and application in band-notched UWB antennas," *IEEE Trans. Antennas Propag.*, vol. 64, no. 9, pp. 3766–3775, Sep. 2016.

[10] Y. Cao, S. W. Cheung, X. L. Sun, and T. I. Yuk, "Frequency-reconfigurable monopole antenna with wide tuning range for cognitive radio," *Microw. Opt. Technol. Lett.*, vol. 56, no. 1, pp. 145–152, 2014.

[11] X. Y. Liu, Y. Fan, and M. M. Tentzeris, "An integrated 'sense-and-communicate' broad-/narrow-band optically controlled reconfigurable antenna for cognitive radio systems," *Microw. Opt. Technol. Lett.*, vol. 57, no. 4, pp. 1016–1023, 2015.

[12] H. Nachouane, A. Najid, F. Riouch, and A. W. Tribak, "Electronically reconfigurable filtenna for cognitive radios," *Microw. Opt. Technol. Lett.*, vol. 59, no. 2, pp. 399–404, 2017.

[13] Q. P-Y, Y. J. Guo, and F. Wei, "A wideband-to-narrowband tunable antenna using a reconfigurable filter," *IEEE Trans. Antennas Propag.*, vol. 63, no. 5, pp. 2282–2285, May 2015.

[14] M.-C. Tang, Z. Wen, H. Wang, M. Li, and R. W. Ziolkowski, "Compact, frequency-reconfigurable filtenna with sharply defined wideband and continuously tunable narrowband states," *IEEE Trans. Antennas Propag.*, vol. 65, no. 10, pp. 5026–5034, Oct. 2017.

[15] J. Deng, S. Hou, L. Zhao, and L. Guo, "Wideband-to-narrowband tunable monopole antenna with integrated bandpass filters for UWB/WLAN applications," *IEEE Antennas Wireless Propag. Lett.*, vol. 16, pp. 2734–2737, 2017.

[16] L. Ge and K. M. Luk, "Band-Reconfigurable Unidirectional Antenna: A simple, efficient magneto-electric antenna for cognitive radio applications," *IEEE Antennas Propag. Mag.*, vol. 58, no. 2, pp. 18–27, Apr. 2016.

[17] M. M. Fakharian, P. A. A. R. Orouji, and M. Soltanpur, "A wideband and reconfigurable filtering slot antenna," *IEEE Ant. Wireless Propag. Lett.*, vol. 15, pp. 1610–1613, 2016.

[18] P.-Y. Qin, A. R. Weily, Y. J. Guo, T. S. Bird, and C.-H. Liang, "Frequency reconfigurable quasi-Yagi folded dipole antenna," *IEEE Trans. Antennas Propag.*, vol. 58, no. 8, pp. 2742–2747, Aug. 2010.

[19] Y. Tawk, J. Costantine, K. Avery, and C. G. Christodoulou, "Implementation of a cognitive radio front-end using rotatable controlled reconfigurable antennas," *IEEE Trans. Antennas Propag.*, vol. 59, no. 5, pp. 1773–1777, May 2011.

[20] T. Aboufoul, A. Alomainy, and C. Parini "Reconfiguring UWB monopole antenna for cognitive radio applications using GaAs FET switches," *IEEE Antennas Wireless Propag. Lett.*, vol. 11, pp. 392–394, 2012.

[21] J. Costantine, Y. Tawk, and C. G. Christodoulou "Motion-activated reconfigurable and cognitive radio antenna systems," *IEEE Antennas Wireless Propag. Lett.*, vol. 12, pp. 1114–1117, 2013.

[22] A. Mansoul, F. Ghanem, M. R. Hamid, and M. Trabelsi, "A selective frequency-reconfigurable antenna for cognitive radio applications," *IEEE Antennas Wireless Propag. Lett.*, vol. 13, pp. 515–518, 2014.

[23] R. Hussain and M. S. Sharawi, "A cognitive radio reconfigurable MIMO and sensing antenna system," *IEEE Antennas Wireless Propag. Lett.*, vol. 14, pp. 257–260, 2015.

[24] J. Y. Siddiqui, C. Saha, and Y. M. M. A. Antar "A novel ultrawideband (UWB) printed antenna with a dual complementary characteristic," *IEEE Antennas Wireless Propag. Lett.*, vol. 14, pp. 974–977, 2015.

[25] F. Martín, J. Bonache, F. Falcone, M. Sorolla, and R. Marqués, "Split ring resonator-based left-handed coplanar waveguide," *Appl. Phys. Lett.*, vol. 83, 22, p. 4652, 2003.

[26] J. Y. Siddiqui, C. Saha, and Y. M. M. Antar, "Compact SRR loaded UWB circular monopole antenna with frequency notch characteristics," *IEEE Trans. Antennas Propag.*, vol. 62, no. 8, pp. 4015–4020, Aug. 2014.

[27] F. Ghanem and P. S. Hall "A bandwidth reconfigurable antenna for cognitive radios," in *Ultra-Wideband, Short Pulse Electromagnetics*, F. Sabath, D. Giri, F. Rachidi, and A. Kaelin, Eds. New York, NY, USA: Springer, 2010, pp. 433–438.

[28] *Ansys HFSS, Version 15*, Ansys, Canonsburg, PA, USA, 2015.

[29] J. Naqui, M. Duran-Sindreu, and F. Martin, "Novel sensors based on the symmetry properties of split ring resonators (SRRs)," *Sensors*, vol. 11, no. 8, pp. 7545–7553, 2011.

[30] M. Barbuto, F. Trotta, F. Bilotti, and A. Toscano, "Horn antennas with integrated notch filters," *IEEE Trans. Antennas Propag.*, vol. 63, no. 2, pp. 781–785, Feb. 2015.